A new methodology for designing heat treated components in fatigue

Etienne Pessard[a]*, Franck Morel[a], Benjamin Abrivard[a-b], Philippe Delhaye[b]

[a] *Arts et Métiers ParisTech, Angers, France*
[b] *Renault SAS, France*

Abstract

This study is dedicated to the effect of the heat treatment on the fatigue strength of an automobile rear axle beam and aims to propose a suitable and reliable methodology for the fatigue design. The rear axle beam is made of sheet metal (22MnB5); the microstructure is initially ferrito-pearlitic before the heat treatment and is martensitic after. A vast experimental campaign has been undertaken to investigate the behaviour, and more specially, the fatigue damage mechanisms observed for both treated and non-treated material, under different loading conditions: tension and shear test with different load ratios. In order to test the sheet metal in shear an original fatigue test apparatus is used.
A probabilistic approach using the weakest link concept is introduced to model the fatigue behaviour. This approach leads naturally to a probabilistic Kitagawa type diagram, which in this case explains the relationship between the influence of the heat treatment and the microstructural heterogeneities.
Integrate in a numerical model, this methodology permit to predict the effect of a local heat treatment on the fatigue strength of the components.

Keywords: Heat treatment, fatigue, self-heating, damage mechanisms, Kitagawa type diagram.

1. Introduction

The 22MnB5 steel, commercially referred to as Usibor 1500 by Arcelor Mittal, has been developed with the aim of reducing the mass of structural components used in the automotive industry. This material is obtained by hot rolling and is characterised by excellent quenchability.

The good quenchability of Boron steels can be taken advantage of by using the Hot Forming Die Quenching process (HFDQ), whereby the sheet metal is austenized and subsequently stamped in a cooled die. [1] To control this process, much research has been devoted to the characterization of the thermo-mechanical behaviour of boron steels [2, 3].

Considerable progress has been made concerning the HFDQ process and it is now possible to vary the final microstructure of a component by optimizing the way in which the tooling is cooled. Some structural components, such as a B-pillar, may benefit from regions that have a lower strength and greater ductility for improved crash performance [4].

Another method of obtaining a heterogeneous microstructure is to manufacture the product by conventional sheet metal forming processes and then to locally quench zones of the component by induction heating. The rear axial beam used in Renault vehicles is a good example of the usefulness of this method. As the axial beam is principally subject to torsional loads, highly loaded zones can be identified (see Fig.1). It is therefore, a priori, not necessary to

* Corresponding author. Tel.: +330241207379
E-mail address: Etienne.pessard@ensam.eu

fully heat treat the entire component as a local heat treatment in certain zones could significantly reduce the manufacturing time.

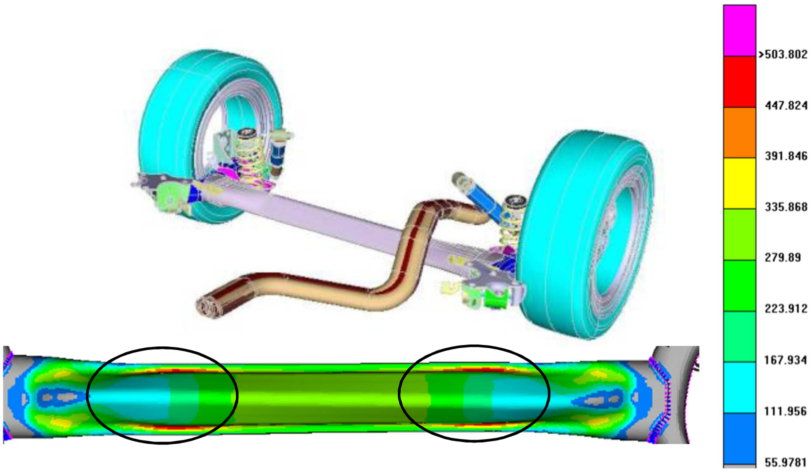

Fig. 1. (a) rear axial beam, (b) Von Mises equivalent stress for torsion loads (from an elastic simulation)

2. The material, 22MnB5 and experimental procedure

The material studied in this work is a ferrito-pearlitic steel commercially referred to as Usibor 1500 and is used to reduce the mass of structural components and reinforcements used in the automotive industry. Its chemical composition is given in Table 1. The material is produced in the form of rolled sheets.

Table 1: Chemical composition of the 22MnB5

Element	C	Mn	Si	P	S	Al	Cr	B	Ti	N	Mo
Weight (%)	**0.206**	**1.191**	0.264	0,019	0,007	0.02	0.199	**0,002**	0.02	-	0,003

The material is isotropic in terms of its mechanical behaviour and its mechanical properties are presented in Table 2. The heat treatment consists of an austenitization at 950 °C for 6 minutes, and then quenching in oil. SEM (Scanning Electron Microscope) observations show a ferrito-pearlitic microstructure in its initial state and martensitic after the heat treatment (see Fig.2)

.

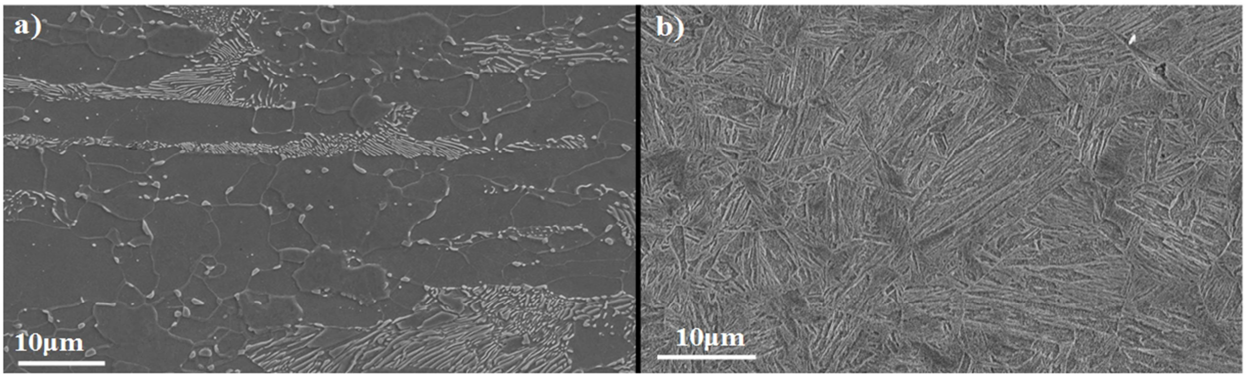

Fig. 2. Microstructure of the 22MnB5 steel, (a) in it initial state, (b) after the heat treatment

Table 2: Mechanical Properties of the 22MnB5 steel

	Ultimate Tensile stress (MPa)	Yield stress (MPa)	Tensile elongation (%)	Superficial hardness HV20
initial state	580	415	25	180
After heat treatment	1300-1650	1000-1250	5	530

For the untreated material, Push-pull (R=-1 and R=0,1) fatigue tests were performed using a vibrophore Rumul testing machine at a frequency of approximately 72 Hz. The fatigue limits were evaluated using the staircase method, at 2x106 cycles using ten specimens per condition.

To define the shearing fatigue limit of the sheet material, an original fatigue test set-up was developed. It is based on the work of [5]. Using a servo-hydraulic fatigue testing machine and the specimen geometry shown in the figure below, it is possible to generate a cyclic pure shear stress state in an area of about 10mm in diameter (see Fig. 3).

With this system, the test frequency is limited. Hence, in order to estimate the high cycle fatigue strength, an accelerated method has been used, that is the self-heating method. These shearing tests were conducted at 10 Hz for load ratios R = -1 and R = 0.1, a single type T thermocouple is fixed to the specimen surface via adhesive tape to measure the temperature. Blocks of 5000 cycles were applied. To estimate the average fatigue limit, the iteration empirical procedure developed by Cura et al. [6] is used.

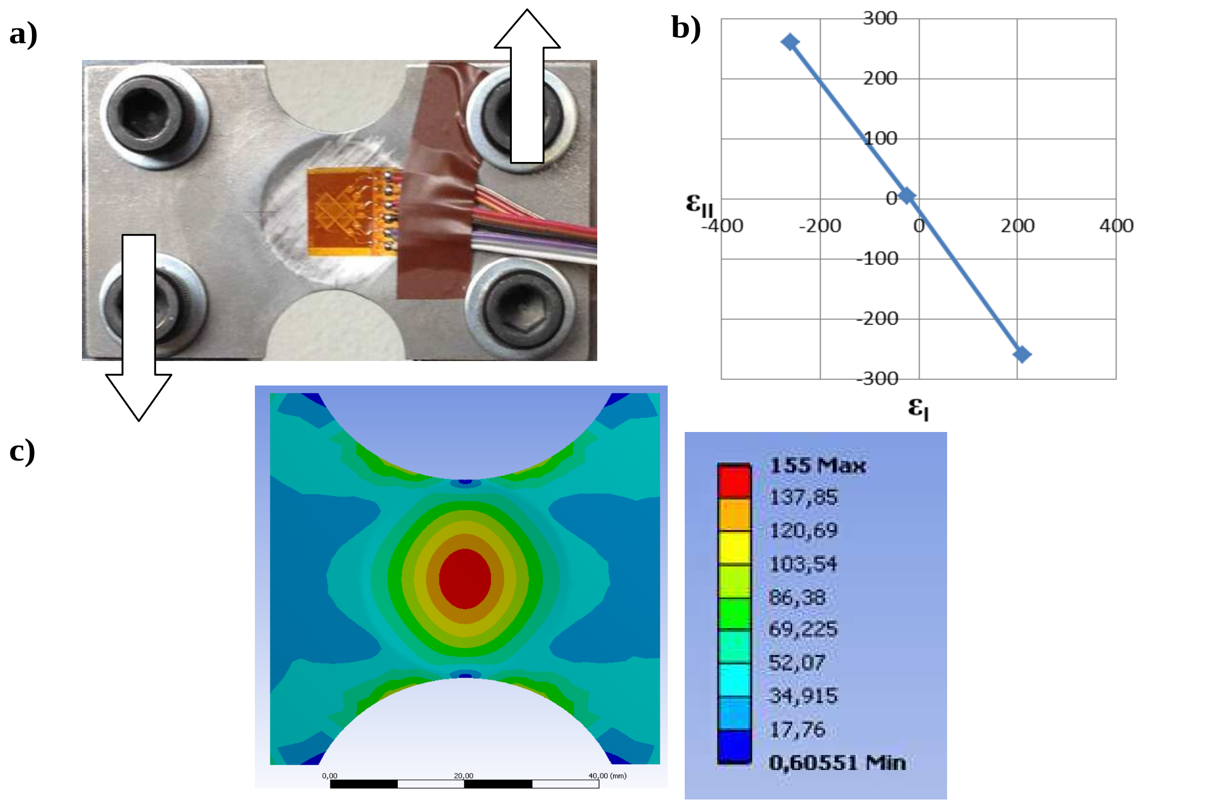

Fig. 3. (a) Picture of the tool (b) Evolution of the two principal deformations during a static loading of tension-compression (c) Von Mises Criterion from an elastic simulation (MPa)

3. Fatigue test results

Table 3 summarized the results of the fatigue test campaign.

Table 3: Fatigue results obtained on the 22MnB5 using staircase method and Self Heating Method (SH test)

		Uniaxial tensile tests	Shear Test
Before Heat Treatment	R=-1	σ=265±5MPa	τ=180MPa (S.H.test)
	R=0,1	σ=230±6MPa	τ=156MPa (S.H.test)
After Heat Treatment	R=-1	σ=626MPa (S.H.test)	x
	R=0,1	σ=400±8MPa σ=394MPa (S.H.test)	x

For the heat treated and non-treated materials, when subject to uniaxial tensile cyclic loads (R = 0.1 and R = -1) fatigue crack initiation most often occurs at alumina inclusions (Al_2O_3) or scratches (see Fig.4). The average size of these inclusions is of the order of 40µm, this value is based on measurement realised on 10 fracture surfaces.

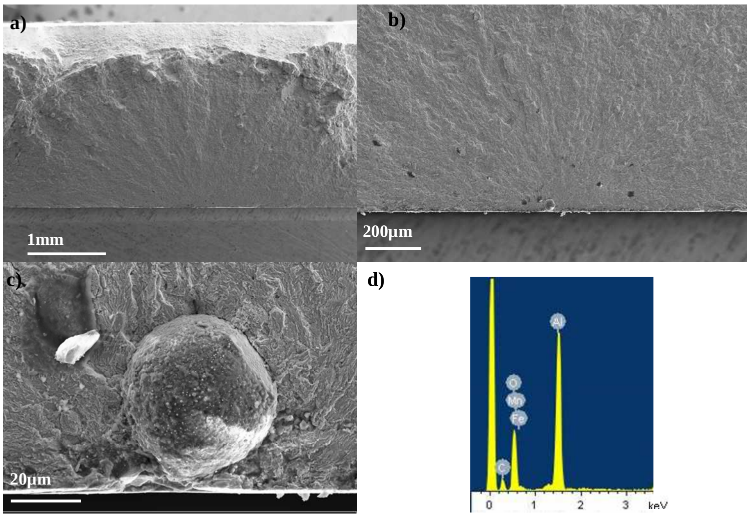

Fig. 4.: (a),(b),(c) Typical failure surfaces, (d) Chemical composition of an inclusion analysed by energy dispersive X-ray spectroscopy

Surface observations of shear specimens shows micro-cracks oriented at 0° and 90° to the specimen axis. This corresponds to the ‘‘classical’’ fatigue crack initiation mechanism in which micro-cracks form on a critical plane (or plane of greatest shear stress amplitude. SEM observations of the failure surfaces (Fig. 5 (b)-(c)) show that the crack initiation sites are not associated with the presence of non-metallic inclusions.

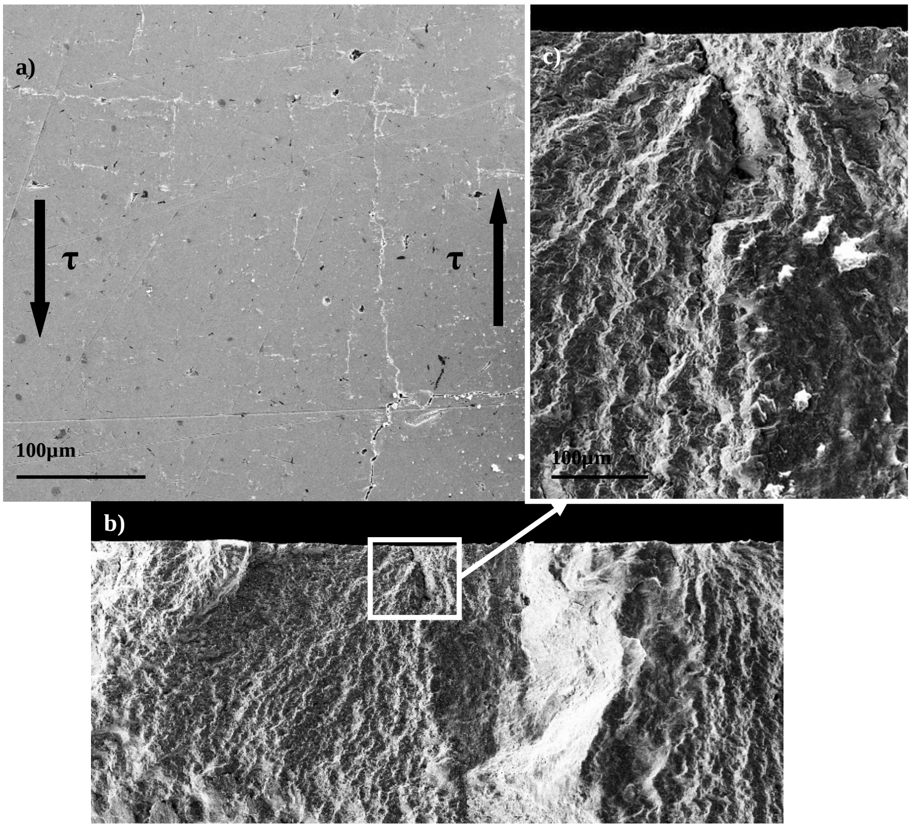

Fig. 5: (a) Observation on the surface of the a shear specimen showing crack initiating in the material matrix at 0° and 90° to the specimen axis, (b-c) failure surfaces of the shear test

Figure 6 shows the results presented in the form of a Dang Van diagram [7]. This high cycle multiaxial fatigue criterion is a critical plane type criterion that is expressed as a linear combination of the shear stress amplitude on the critical plane and of the maximum hydrostatic stress. The fatigue limit values for the non-treated material form a straight line in this diagram. This line corresponds to the Dang Van criterion, usually used for ductile materials.

Given the hardness of our material and the average defect size, it is possible to use the Murakami [8] criterion to predict fatigue limits for each loading condition. These predictions are plotted in Fig. 6. The Murakami [8] criterion uses the parameter $\sqrt{area}$ (where area is the projected area of a defect) and the hardness to define the fatigue strength via the following equation:

$$\sigma_w = \frac{A(H_v + 120)}{\left(\sqrt{area}\right)^{1/6}} \left(\frac{1-R}{2}\right)^{\alpha} \quad (1)$$

Where $\alpha = 0.226 + H_v \times 10^{-4}$ and $A = 1.43$ or 1.56 for surface and internal defects, respectively for torsional loads and surface defects, the fatigue strength can be expressed as:

$$\sigma_w = \frac{0.93(H_v + 120)}{F(b/a)\left(\sqrt{area}\right)^{1/6}} \left(\frac{1-R}{2}\right)^{\alpha} \quad (2)$$

where $F(b/a) = 0.8397$ for spherical defects.

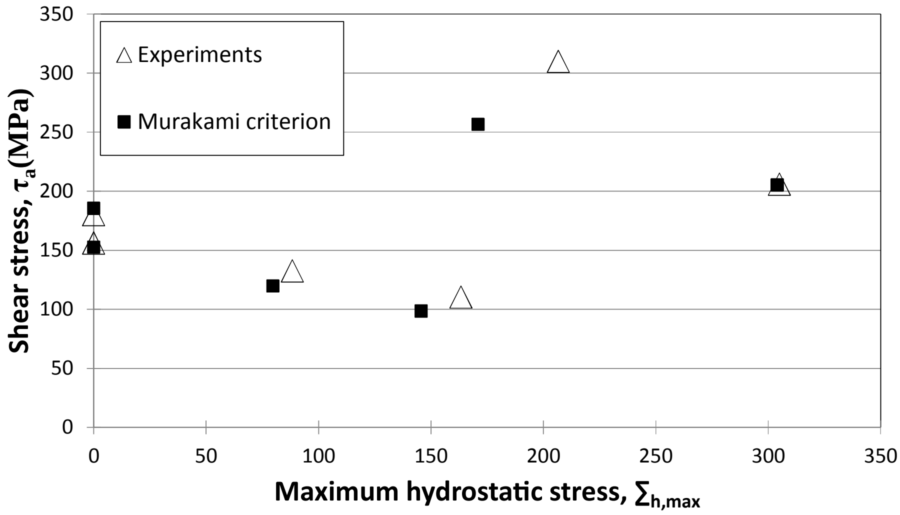

Fig.1: Dang Van diagram, showing the Murakami predictions and the corresponding data for the 22MnB5 steel

It can be seen that the Murakami criterion is able to accurately predict the fatigue limit of the untreated material in tension and shearing with R=0.1 and R=-1. This result is surprising because despite the fact that the damage mechanism observed in shear is not associated with the presence of a defect, the Murakami criterion results in good predictions. Concerning the heat treated material, the Murakami criterion is however less accurate for tensile loads with a R-ratio of 0.1. This hypothesis, of the existence of two fatigue damage mechanisms, depending on the type of loading condition, will be the basis of the proposed modelling approach.

The proposed modelling framework is a flexible way of taking into account multiple, coexisting, fatigue damage mechanisms via the combination of two appropriate high cycle fatigue criteria. One criterion to model fatigue damage associated with crack initiation and a second for crack propagation (or crack arrest).

4. A probabilistic multiaxial fatigue criterion and kitagawa diagram for the 22MnB5 steel

In order to model both fatigue crack initiation and propagation the model developed by Pessard et al. [9, 10] is used. It permits to combine the Papadopoulos [11] and classical LEFMS models. The threshold defined by each one of these criteria is then re-defined in terms of a Weibull distribution, giving a failure probability caused by each of these mechanisms.

The total probability of survival of the component is defined by applying the weakest link hypothesis. It is obtained by multiplying the two survival probabilities from the two different observed mechanisms:

	Mechanism 1	Mechanism 2
threshold	$\sigma_{eq} < \sigma_{th}$	$\Delta K < \Delta K_{th}$
Probability density function	$f_{01}(\sigma_{th}) = \frac{m_1}{\sigma_{th01}} \left(\frac{\sigma_{th}}{\sigma_{th01}} \right)^{m_1 - 1} \exp - \left(\frac{\sigma_{th}}{\sigma_{th01}} \right)^{m_1}$	$f_{02}(\Delta K_{th}) = \frac{m_1}{\Delta K_{th02}} \left(\frac{\Delta K_{th}}{\Delta K_{th02}} \right)^{m_2 - 1} \exp - \left(\frac{\Delta K_{th}}{\Delta K_{th02}} \right)^{m_2}$
Failure probability	$P_{F_1} = 1 - \exp\left[-\frac{1}{S_{01}} \int_{S_{\Omega 1}} \left(\frac{\sigma_{eq}}{\sigma_{th01}} \right)^{m1} dS \right]$	$P_{F_2} = 1 - \exp\left[-\frac{1}{S_{02}} \int_{S_{\Omega 2}} \left(\frac{\Delta K}{\Delta K_{th02}} \right)^{m2} dS \right]$

Total failure probability	$P_F = 1 - \exp\left\{ - \left[\frac{S_{\Omega 1}}{S_{01}} \left(\frac{\sigma_{eq}}{\sigma_{th01}} \right)^{m1} + \frac{S_{\Omega 2}}{S_{02}} \left(\frac{\Delta K}{\Delta K_{th02}} \right)^{m2} \right] \right\}$

For example, for traction-compression loads, the Papadopoulos [11] criterion can be written as:

$$\sigma_{eq} = \sqrt{\langle T_a \rangle} + k\sigma_{H,\max} = \left(\frac{1}{2} + \frac{2k}{3(1-R)} \right) \sigma_{I,a} \tag{3}$$

and the Murakami criterion can be written as :

$$\Delta K = 0.65\sigma_{I,a}\sqrt{\pi\sqrt{area}} \text{ and } \Delta K_{th} = 3.3\times10^{-3}(H_v+120)\left(\sqrt{area}\right)^{1/3}\left(\frac{1-R}{2}\right)^{\alpha} \tag{4}$$

By assuming that the scatter is the same for both mechanisms, $m = m_1 = m_2$ that there is no scale effect $\left(\frac{S_{\Omega 1}}{S_{01}} = \frac{S_{\Omega 2}}{S_{02}} = 1 \right)$ and the defects have a spherical shape, the traction-compression fatigue limit can be written as:

$$\sigma_{I,a}(P_F, a) = \left[\frac{\ln\left(\frac{1}{1-P_F} \right)}{\left(\frac{\sigma_{eq}}{\sigma_{th01}} \right)^m + \left(\frac{\Delta K}{\Delta K_{th02}} \right)^m} \right]^{\frac{1}{m}} \tag{5}$$

Plotting the fatigue limit as a function of the defect size it is possible to obtain a Kitagawa type diagram (Fig.7).
In order to take into account the effect of the heat treatment, it is necessary to make both thresholds σ'_{th01} and C'_{th02} a function of the heat treatment. As well, for the Murakami criterion, it is proposed to make both thresholds depend on the hardness.

$$\sigma_{th01} = A(H_v + 120) \text{ and } \Delta K_{th02} = B(H_v + 120) \tag{6}$$

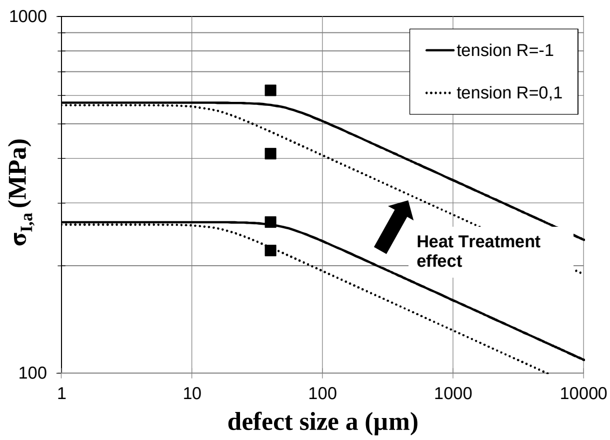

Fig. 7: Relationship between hardness and fatigue limit

This is a strong assumption that is proposed in order to demonstrate the possibilities of the proposed model. The aim is to develop an approach that is both phenomenological and empirical, which can be applied to the industrial problem of applying a local heat, the results of which are currently measured in terms of hardness. It is necessary to undertake a larger testing program in order to identify each one of these relationships. The predictions from the proposed model are shown in a Kitagawa's diagram (Fig. 7).

5. Conclusion

The fatigue behaviour of the 22MnB5 steel has been characterized for different loading conditions and heat treatments. For this, an original shearing test setup has been employed to determine the fatigue behaviour of the 22MnB5 steel in shear. An original modelling approach has been developed to take into account the evolution of the fatigue behaviour depending on the applied heat treatment.

References

[1] H. Karbasian, A.E. Tekkaya, A review on hot stamping, Journal of Materials Processing Technology 210 (2010) 2103–2118.

[2] H. Liu, Hot formation quality of high strength steel BR1500HS for hot stamping without cooling system, Trans. Nonferrous Met. Soc. China 22(2012) s542−s547.

[3] A. Bardelcik, Effect of cooling rate on the high strain rate properties of boron steel, International Journal of Impact Engineering 37 (2010) 694–702.

[4] M. Merklein, Investigation of the thermo-mechanical properties of hot stamping steels, Journal of Materials Processing Technology 177 (2006) 452–455.

[5] A. Galtier et B. Weber, Fatigue tests on thin sheet materials, fatigue design 2005.

[6] F. Cura, G. Curti, R. Sesana, Int. J. Fatigue 27 (2005) 453–459.

[7] K. DangVan, Sur la résistance en fatigue des métaux, Sci Tech Armement, 1973, 47

[8] Y. Murakami Metal fatigue effects of small defects and non-metallic inclusions, Elesvier 2002

[9] Pessard E., Bellett D., Morel F., Koutiri I., A mechanistic approach to the Kitagawa-Takahashi diagram using a multiaxial probabilistic framework, Eng.Fract. Mech., (2013),vol. 109, pp. 89-104

[10] E. Pessard, F. Morel, A. Morel, D. Bellett, Modelling the role of non-mettalic inclusions on the anisotropic fatigue behaviour of forged steel, Int. J. Fatigue 33-4 (2011) 568-577

[11] I.V Papadopoulos., Fatigue limit of metals under multiaxial stress conditions: the microscopic approach, ISEI/IE 2464/93, Commission of the European Communities Joint Research Center, 1993